Transition Metal Complexes of 12- and 13-Membered Functionalized Macrocycles, Dioxotetraazacycloalkanediacetates

Michiko B. Inoue,[†,‡] Paul Oram,[‡] Gabriel Andreu-de-Riquer,[†,§] Motomichi Inoue,*[,†] Peter Borbat,[‡] Arnold Raitsimring,[‡] and Quintus Fernando[‡]

CIPM, Universidad de Sonora, Apartado Postal 130, Hermosillo, Sonora, Mexico, and Department of Chemistry, University of Arizona, Tucson, Arizona 85721

Received November 30, 1994[⊗]

Formation constants of Mn^{2+}, Co^{2+}, Ni^{2+}, Cu^{2+}, and Zn^{2+} complexes formed in aqueous solutions with 12-membered and 13-membered macrocycles have been determined, and the solution electronic spectra have been studied. The 12-membered macrocycle, abbreviated as (12edtaen)H_2, is 2,9-dioxo-1,4,7,10-tetraaza-4,7-cyclododecanediacetic acid, and the 13-membered macrocycle, abbreviated as (13edtapn)H_2, is 2,9-dioxo-1,4,7,10-tetraaza-4,7-cyclotridecanediacetic acid. The structures of $[Zn(C_{12}H_{18}N_4O_6)]\cdot 4H_2O$ and $[Mn(C_{13}H_{20}N_4O_6)(H_2O)]_2\cdot 7H_2O$ have been determined by single-crystal X-ray analyses. The zinc complex crystallized in the monoclinic space group $P2_1/n$ with $a = 10.205(2)$ Å, $b = 9.599(2)$ Å, $c = 19.431(3)$ Å, $\beta = 100.268\ (2)°$, and $Z = 4$. The coordination geometry around the zinc atom is distorted octahedral with five donor atoms (two amine nitrogen, an amide oxygen, and two acetate oxygen atoms) from one ligand molecule and an acetate oxygen atom from a neighboring zinc chelate. The zinc atoms are linked by Zn−O−C−O−Zn bonds and form a one-dimensional array. The manganese complex crystallized in the orthorhombic space group *Pccn* with $a = 16.325(1)$ Å, $b = 17.468(1)$ Å, $c = 15.144(1)$ Å, and $Z = 4$. The coordination geometry around the manganese atom is a highly distorted trigonal prism with five donor atoms from a ligand molecule and an oxygen atom from a water molecule. The formation constants of the ML species of Ni^{2+} and Cu^{2+} with $(12edtaen)^{2-}$ are significantly higher than those of the corresponding complexes with $(13edtapn)^{2-}$. The MLH_{-2} species of Co^{2+}, Ni^{2+}, and Cu^{2+} formed with $(13edtapn)^{2-}$ in the basic region have greater formation constants than the corresponding MLH_{-1} species. The solution electronic spectra of the MLH_{-2} species of these complexes are quite different from those of the corresponding ML species, indicating that conversion of coordination geometry occurs as a result of deprotonation of amide nitrogen atoms. This conversion has been confirmed by an electron spin echo envelope modulation experiment for the Cu^{2+} complex. No significant spectral changes are observed with the M(12edtaen) complexes. In these complexes the mixed-ligand complexes, M(12edtaen)$(OH)_n$ ($n = 1$ or 2), are formed in the basic region, and the complexes with $n = 2$ are much less stable than the corresponding complexes with $n = 1$. These large differences in the properties of the metal complexes of the two macrocyclic ligands are caused by a difference of only one $-CH_2-$ group in the ligand ring system.

Introduction

Selective complexation of macrocyclic ligands with specific metal ions is an important and rapidly expanding area of research.[1] Our work in this field has been directed primarily toward the synthesis and characterization of a series of macrocyclic ligands with 12-membered to 24-membered ring systems. In the course of our previous work we have reported that a condensation reaction between ethylenediaminetetraacetic (edta) dianhydride and ethylenediamine (en) or 1,3-diaminopropane (pn) gives a 12-membered or 13-membered macrocycle, (12edtaen)H_2 (**I**) or (13edtapn)H_2 (**II**), which contains two amide groups in the ring system and two pendant carboxymethyl groups.[2,3] The new macrocyclic ligands incorporate three types of coordinating atoms (amine nitrogen, amide oxygen, and acetate oxygen atoms), which have different coordination abilities. This feature in the ligand is expected to result in high selectivity toward specific metal ions, and the resulting metal chelates are expected to have novel physical and structural properties. In this work, we have determined the formation constants of the 12-membered and the 13-membered macrocycles with divalent transition metal ions, Mn^{2+}, Co^{2+}, Ni^{2+}, Cu^{2+}, and Zn^{2+}. The coordination properties of the 12-membered and 13-membered ligands toward Co^{2+}, Ni^{2+} and Cu^{2+} ions are significantly different, even though their ring sizes differ by only one $-CH_2-$ group. In order to confirm these novel properties, we have studied electronic spectra of these complexes and single-crystal X-ray structures of two selected metal complexes.

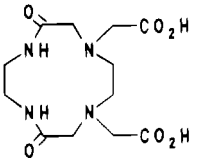

I 12(edtaen)H_2

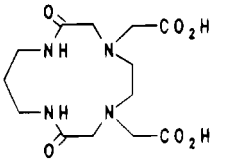

II 13(edtapn)H_2

[†] Universidad de Sonora.

[‡] University of Arizona.

[§] On leave from the Instituto de Investigaciones Científicas, Universidad de Guanajuato, Guanajuato, Guanajuato, Mexico.

[⊗] Abstract published in *Advance ACS Abstracts,* June 1, 1995.

(1) (a) Izatt, R. M., Christensen, J. J., Eds. *Synthesis of Macrocycles, The Design of Selective Complexing Agents*; Progress in Macrocyclic Chemistry Vol. 3; John Wiley & Sons: New York, 1987. (b) Izatt, R. M.; Pawlak, K.; Bradshaw, J. S.; Bruening, R. L. *Chem. Rev.* **1991**, *91*, 1721. (c) van Veggel, F. C. J. M.; Verboom, W.; Reinhoudt, D. N. *Chem. Rev.* **1994**, *94*, 279. (d) Hancock, R. D. *J. Chem. Educ.* **1992**, *69*, 615.

(2) Inoue, M. B.; Villegas, C. A.; Asano, K.; Nakamura, M.; Inoue, M.; Fernando, Q. *Inorg. Chem.* **1992**, *31*, 2480.

(3) Inoue, M. B.; Fernando, Q.; Villegas, C. A.; Inoue, M. *Acta Crystallogr. C* **1993**, *49*, 875.

0020-1669/95/1334-3528$09.00/0

Table 1. Analytical Data, Magnetic Moments μ at 300 K, and Absorption Maxima λ of Aqueous Solution Electronic Spectra

	anal.: found, % (calcd, %)				
	C	H	N	μ, μ_B	λ, nm
Mn(12edtaen)·2.5H$_2$O	34.58 (34.79)	5.10 (5.60)	13.31 (13.53)	5.8	
Mn(13edtapn)·4H$_2$O	34.24 (34.29)	5.30 (5.76)	12.27 (12.31)	5.9	
Co(12edtaen)·H$_2$O	36.54 (36.83)	4.92 (5.15)	14.16 (14.32)	4.7	490, 510
Co(13edtapn)·3H$_2$O	35.16 (35.38)	5.54 (5.94)	12.66 (12.70)	4.8	510
Ni(12edtaen)·4H$_2$O	32.40 (32.38)	5.26 (5.89)	12.46 (12.59)	3.20	380, 607, 1020
Ni(13edtapn)·2H$_2$O	36.44 (36.91)	5.78 (5.72)	12.99 (13.24)	3.14	380, 605, 1020
Cu(12edtaen)·H$_2$O	36.39 (36.41)	4.71 (5.09)	13.95 (14.15)	1.93	745
Cu(13edtapn)·H$_2$O	38.50 (38.09)	5.13 (5.41)	13.83 (13.67)	1.92	700
Zn(12edtaen)·4H$_2$O	32.36 (31.91)	5.17 (5.80)	12.36 (12.41)		
Zn(13edtapn)·3H$_2$O	34.31 (34.88)	5.50 (5.86)	12.42 (12.52)		

Table 2. Crystallographic Data for Zn(12edtaen) and Mn(13edtapn)

	Zn(12edtaen)	Mn(13edtapn)
chem formula	[Zn(C$_{12}$H$_{18}$N$_4$O$_6$)]·4H$_2$O	[Mn(C$_{13}$H$_{20}$N$_4$O$_6$)(H$_2$O)]$_2$·7H$_2$O
fw	451.73	928.67
space group	$P2_1/n$ (No. 14)	*Pccn* (No. 56)
a, Å	10.205(2)	16.325(1)
b, Å	9.599(2)	17.468(1)
c, Å	19.431(3)	15.144(1)
β, deg	100.268(2)	
V, Å^3	1872.9(9)	4318.5(7)
Z	4	4
T, °C	22	22
λ, Å	0.710 73	0.710 73
ϱ_{calcd}, g cm^{-3}	1.60	1.43
μ, cm^{-1}	14.0	6.4
R[a]	0.028	0.074
R_w[b]	0.042	0.095

[a] $R = \Sigma|F_o - F_c|/\Sigma F_o$. [b] $R_w = [\Sigma w(F_o - F_c)^2/\Sigma wF_o^2]^{1/2}$.

Experimental Section

Syntheses of Materials. The macrocyclic ligands were synthesized by the methods reported previously.[2,3] Their purity was checked by ^{1}H NMR.[4] The metal complexes were prepared by reaction between the ligands and a metal carbonate in excess at approximately 40 °C. The excess carbonate was removed by filtration, and the filtrate was concentrated. When the resulting solution was mixed with ethanol, the complex was precipitated. The product was purified by precipitation from aqueous solutions by the addition of ethanol or acetone. Table 1 shows the analytical data, which were obtained by Desert Analytics, Tucson, AZ.

X-ray Crystal Analyses. Single-crystal X-ray analyses were carried out on [Zn(12edtaen)]·4H$_2$O and [Mn(13edtapn)(H$_2$O)]$_2$·7H$_2$O. The crystallographic data are summarized in Table 2. Scattering factors were taken from Cromer and Waber.[5] All calculations were performed on a VAX computer with the program package MolEn.[6]

Colorless platelike crystals of [Zn(12edtaen)]·4H$_2$O were obtained by diffusion of acetone into an aqueous solution of the compound. A crystal of approximate dimensions 0.41 × 0.40 × 0.21 mm was mounted on a Syntex P2$_1$ diffractometer with a Crystal Logics computer control system. A total of 3710 reflections ($+h,+k,\pm l$) with maximum 2θ of 50° were collected with monochromated Mo Kα radiation; 3298 reflections were unique with R_{int} = 0.013; 2452 reflections with $I > 3\sigma_I$ were used in the refinements. An empirical absorption correction based on a Ψ-scan was calculated using the program ABSCOR. The transmission factors were ranged from 0.832 to 1.000. The position of a zinc atom was revealed by the Patterson heavy-atom method. The remaining atoms were located in succeeding difference Fourier syntheses. When all the non-hydrogen atoms were located, most hydrogen atoms were visible in the difference map: hydrogen atoms of water molecules were located from the difference map. Hydrogen atoms bonded to carbon and nitrogen atoms were placed at the idealized positions with a bond length of 0.95 Å. Hydrogen atoms were included in the refinement but constrained to ride on the atoms to which they are bonded. The final refinement converged at R = 0.028 with 244 parameters. The maximum and minimum peaks in the final difference map were 0.30 and −0.12 e Å^{-3}, respectively.

Colorless needle crystals of [Mn(13edtapn)(H$_2$O)]$_2$·7H$_2$O were obtained by slow evaporation from an aqueous solution of the complex. A crystal of dimensions 0.33 × 0.10 × 0.08 mm was mounted on an Enraf-Nonius CAD4 diffractometer. A total of 4253 reflections ($+h,+k,+l$, $0 < 2\theta < 50°$) were collected with monochromated Mo Kα radiation; 3801 reflections were unique and not systematically absent; 1692 reflections with $I > 3\sigma_I$ were used in the refinements. No absorption correction was made. The structure was solved by direct methods; 24 atoms were located from an E-map. The remaining atoms were located in succeeding difference Fourier syntheses. Hydrogen atoms were included in the refinement with riding model. For water oxygen Ow5 and Ow6, the temperature factors (B_{eq}) were ~20 Å^2 with full occupancy; these atoms were, therefore, refined by assuming a half-occupancy. In the final difference Fourier map the highest peak amounting to 1.5 e Å^{-3} remained near Ow5 and Ow6. This suggested that each of these water molecules was disordered between the two positions with fractional occupancies; however, such a disorder was not modeled. The disorder of water molecules as well as the small size of the crystal resulted in a relatively large R factor of 0.074 (267 parameters).

Formation Constants. The formation constants of the transition metal complexes were determined by a potentiometric method. A 0.1 M potassium hydroxide solution was made from a filtered 50% (w/v) stock solution in distilled deionized water that was boiled and cooled under nitrogen before use. The solution was kept under nitrogen in the reservoir of a 5 mL buret and was standardized with 99.95% potassium hydrogeniodate (G. Frederick Smith). Stock solutions of metal chlorides (approximately 0.05 M) were prepared and standardized by titration with edta.[7,8] The ligands were dried for at least 12 h at 90 °C before use. Approximately 0.05 M stock solutions of the ligands were prepared and their concentrations, together with the acid dissociation constants of the ligands, were determined by titration with standard KOH and by using the program PKAS.[9] The acid dissociation constants agreed with the values reported previously within experimental error.[4]

Potentiometric titrations were carried out in a sealed jacketed vessel under nitrogen at 25 °C with a Beckman Model Phi 72 pH meter equipped with a Corning 476280 glass electrode and a Corning 476350 calomel reference electrode. A 1 mm i.d. Teflon tube containing agarose saturated with KCl was used as a salt bridge between the reference electrode and the titration vessel. A standard 0.1000 M hydrochloric acid (Ricca) was titrated with a standard solution of KOH. A plot of measured pH *versus* calculated values of −log [H$^+$] gave straight lines in the acidic and basic regions which could be used to convert measured pH values to hydrogen ion concentrations. All titrations were carried out in 0.1 M KCl.

It was necessary to carry out at least two types of titrations, because the formation constants of most of the metal complexes were so high that titration of a metal−ligand mixture alone gave indeterminate results. The formation constants for ML species were determined by competitive titrations with tris(2-aminoethyl)amine (tren) as a competing ligand:[10] the sample solutions contained approximately 0.05 mmol of each analyte. The formation constants of MLH$_{-n}$ species were determined by titrations in which only the metal and the ligand (approximately

(4) Inoue, M. B.; Oram, P.; Inoue, M.; Fernando, Q. *Inorg. Chim. Acta* **1995**, *232*, 91.
(5) Cromer, D. T.; Waber, J. T. *International Tables for X-ray Crystallography*; The Kynoch Press: Birmingham, England, 1974; Vol. IV, Table 2.2B.
(6) Fair, C. K. *MolEn. An Interactive Intelligent System for Crystal Structure Analysis*; Enraf-Nonius: Delft, The Netherlands, 1990.
(7) Přibil, R. *Applied Complexometry*; Pergamon Press: Oxford, U.K., 1982.
(8) Fritz, J. S.; Oliver, R. T.; Pietrzyk, D. J. *Anal. Chem.* **1958**, *30*, 1111.
(9) Martell, A. E.; Motekaitis, R. J. *Determination and Use of Stability Constants*; VCH: New York, 1992.
(10) Ackermann, H.; Schwarzenbach, G. *Helv. Chim. Acta* **1949**, *32*, 1543.

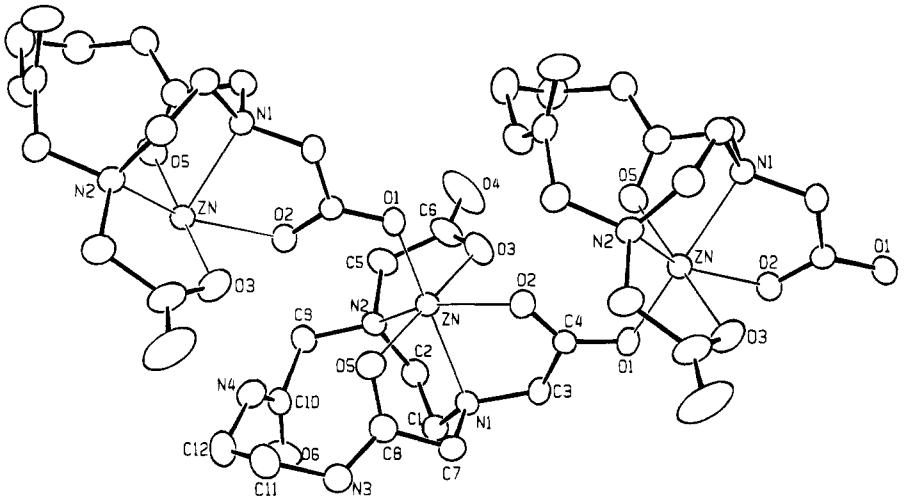

Figure 1. Structure of $[Zn(12edtaen)]_n$. The atoms are shown at the 50% probability level.

0.1 mmol each) were present. This titration was necessary, because the presence of tren depressed the formation of these species at high pH values. For some metal complexes, edta was used as the competing ligand, but it presented some difficulties that have been pointed out previously.[11] All formation constant calculations were performed by using the program BEST.[9]

Spectroscopic and Magnetic Measurements. The UV−visible spectra of the complexes in aqueous solutions were obtained with a Hewlett Packard 8452A diode array spectrophotometer and a Perkin-Elmer Lambda 2 spectrophotometer.

The magnetic susceptibilities of the solid complexes were determined by using a Faraday balance at a field strength of 6 kG. The standard used was copper(II) sulfate pentahydrate (5.85×10^{-6} emu g^{-1} at 300 K), which was calibrated with 99.99% sodium chloride (Tomita Seiyaku) (-0.520×10^{-6} emu g^{-1}).[12] The molar susceptibilities were corrected for diamagnetic contributions from $(12edtaen)H_2$ (-199×10^{-6} emu mol^{-1}), $(13edtapn)H_2$ (-211×10^{-6}) and water (-13×10^{-6}): the diamagnetic susceptibilities of the ligands were calculated on the basis of the Pascal constants.[12] No correction was made for the diamagnetism of metal ions. The magnetic moments (in Bohr magnetons) were calculated by $\mu = 2.83(\chi T)^{1/2}$ (χ = corrected molar magnetic susceptibility in emu mol^{-1}); the contribution of the temperature-independent paramagnetism was not taken into account.

Continuous-wave electron spin resonance (CW ESR) and electron spin echo envelope modulation (ESEEM) experiments were performed for Cu(13edtapn) in acidic and basic matrices. For the continuous-wave spectra, an acid solution was prepared by dissolving approximately 10^{-2} M $CuCl_2$ and $(13edtapn)H_2$ in 50% methanol (pH ~ 2), and a basic solution (pH ~ 13) was made by the addition of KOH to the acidic solution. For the spin echo experiments, 0.05 M acidic and basic solutions were prepared likewise. The CW ESR spectra were taken at frequencies of 9.2763 and 9.2795 GHz at liquid nitrogen temperature on a Bruker ESP-300 spectrometer. The microwave frequency was controlled by a Systron-Donner 6530 microwave counter to assure accurate determination of g values. The spin echo experiments were performed on a laboratory-built X, P band ESE spectrometer.[13] The sample temperature was controlled at a temperature between 4.2 and 10 K with an Oxford ESR-900 helium flow low-temperature accessory, which was placed into a TE102 X-band cavity. For selected field positions in the ESR spectra of the acidic and basic solutions, two- and three-pulse ESEEM patterns were recorded. For the two-pulse experiment, a sequence of 30 ns $2\pi/3$ pulses with an initial separation by 300 ns was used. For the stimulated ESE experiment, an eight-phase step sequence of three $\pi/2$ pulses of 30 ns duration was used to eliminate unwanted primary echoes.[14] Stimulated ESEEM patterns were recorded for a set of τ (interval between the first and the second pulses) in the range 300−1000 ns and T (interval between the second and the third pulses) starting at 50 ns.

Table 3. Fractional Coordinates and Equivalent Isotropic Temperature Factors of $[Zn(12edtaen)]\cdot 4H_2O$

atom	x	y	z	B_{eq},[a] Å^2
Zn	0.32153(3)	0.01482(3)	0.21888(2)	1.885(6)
O1	0.2490(2)	−0.4035(2)	0.2010(1)	3.02(5)
O2	0.2248(2)	−0.1810(2)	0.2283(1)	2.27(4)
O3	0.4825(2)	−0.0800(2)	0.2844(1)	3.13(5)
O4	0.6803(3)	−0.0318(3)	0.3484(2)	5.84(7)
O5	0.1596(2)	0.1123(2)	0.1513(1)	2.58(4)
O6	0.4404(2)	0.2988(3)	0.0431(1)	3.19(5)
N1	0.3306(2)	−0.0887(2)	0.1200(1)	1.84(4)
N2	0.4986(2)	0.1323(2)	0.1929(1)	1.95(5)
N3	0.1008(3)	0.1550(3)	0.0354(1)	2.57(5)
N4	0.2858(3)	0.3609(3)	0.1078(1)	2.71(5)
C1	0.4379(3)	−0.0243(3)	0.0881(1)	2.23(6)
C2	0.5488(3)	0.0345(3)	0.1432(2)	2.31(6)
C3	0.3516(3)	−0.2359(3)	0.1400(2)	2.19(6)
C4	0.2681(3)	−0.2751(3)	0.1941(1)	2.04(5)
C5	0.5918(3)	0.1304(3)	0.2617(2)	2.79(6)
C6	0.5842(3)	−0.0054(4)	0.3008(2)	3.18(7)
C7	0.1998(3)	−0.0683(3)	0.0745(2)	2.25(6)
C8	0.1513(3)	0.0749(3)	0.0889(2)	2.22(6)
C9	0.4976(3)	0.2808(3)	0.1687(2)	2.35(6)
C10	0.4037(3)	0.3130(3)	0.1001(2)	2.22(6)
C11	0.0619(3)	0.2994(3)	0.0464(2)	3.04(7)
C12	0.1790(3)	0.3978(3)	0.0508(2)	3.20(7)
Ow1	0.8362(3)	0.2026(3)	0.3973(1)	4.62(6)
Ow2	0.7795(3)	0.7966(3)	0.4622(1)	5.66(7)
Ow3	0.6310(3)	0.3969(3)	0.3979(1)	5.39(7)
Ow4	0.5995(3)	0.6282(4)	0.3066(2)	7.90(9)

[a] $B_{eq} = (4/3)[a^2\beta_{1,1} + b^2\beta_{2,2} + c^2\beta_{3,3} + ab(\cos\gamma)\beta_{1,2} + ac(\cos\beta)\beta_{1,3} + bc(\cos\alpha)\beta_{2,3}]$.

Results

Structure of $[Zn(12edtaen)]\cdot 4H_2O$. Figure 1 shows the structure of the Zn chelate, which crystallized in the monoclinic space group $P2_1/n$. The positional parameters are collected in Table 3, and selected bond distances and X−Zn−Y bond angles are shown in Table 4. A zinc atom is coordinated to two carboxylate oxygen atoms, two amine nitrogen atoms, and an amide oxygen atom from a ligand molecule. In addition, a carboxylate oxygen atom from an adjacent metal chelate molecule is coordinated to the metal atom with the shortest Zn−X distance. The resulting coordination geometry around the central metal ion is a distorted octahedron. A carboxylate group bridges two metal ions, leading to the formation of a one-dimensional −Zn−O−C−O−Zn− array. This polymeric struc-

(11) Schwarzenbach, G.; Freitag, E. *Helv. Chim. Acta* **1951**, *34*, 1503.
(12) Foëx, F. *Constantes Sélectionnées Diamagnétisme et Paramagnétisme*; Masson: Paris, 1957.
(13) Borbat, P.; Raitsimring, A. *36th Rocky Mt. Conf. Anal. Chem., EPR Symp.* **1994**, 94.
(14) Fauth, J.-M.; Schweiger, A.; Braunschweiler, L.; Forrer, J.; Ernst, R. R. *J. Magn. Reson.* **1986**, *66*, 74.

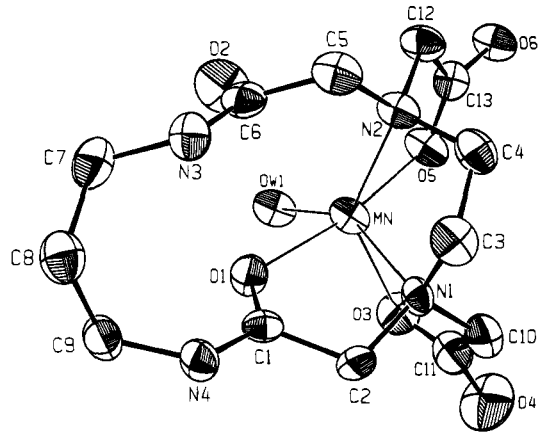

Figure 2. Molecular structure of [Mn(13edtapn)(H_2O)]. The atoms are shown at the 50% probability level.

Table 4. Selected Bond Distances (Å) and Angles (deg) for [M(12edtaen)]·4H_2O (M = Zn or Cu)

	Zn	Cu[a]
M−O1′$_{carboxylate}$	1.989(2)	1.936(4)
M−O2$_{carboxylate}$	2.146(2)	2.334(3)
M−O3$_{carboxylate}$	2.098(2)	1.996(4)
M−O5$_{amide}$	2.135(2)	1.988(4)
M−N1$_{amine}$	2.179(2)	2.088(4)
M−N2$_{amine}$	2.262(2)	2.485(4)
N3$_{amide}$−C8	1.322(4)	1.311(7)
N3$_{amide}$−C11	1.468(4)	1.471(7)
N4$_{amide}$−C10	1.321(4)	1.305(8)
N4$_{amide}$−C12	1.452(4)	1.469(8)
N1−M−O1′	161.40(9)	168.7(2)
O2−M−N2	148.60(8)	142.9(1)
O3−M−O5	179.21(9)	177.1(2)

[a] Reference 2.

ture resembles the structure of the Cu(12edtaen)·4H_2O, which crystallized in the orthorhombic space group $P2_12_12_1$.[2] Table 4 includes bond distances and angles of the copper(II) complex for comparison. In the Cu complex, the octahedron is elongated along O2−Cu−N2 bonds. Such an elongation is not found in the zinc(II) complex. The elongated octahedron in the copper(II) compound is dominated by the Jahn−Teller distortion effect rather than by the conformation of the ligand molecule.

Structure of [Mn(13edtapn)(H_2O)]$_2$·7H_2O. The molecular structure of the complex is shown in Figure 2. The positional parameters are collected in Table 5, and selected bond distances are in Table 6. A Mn^{2+} ion is coordinated to two amine nitrogen atoms, two carboxylate oxygen atoms, and one amide oxygen atom from a ligand molecule. A water molecule occupies the sixth coordination site. The resulting coordination polyhedron is a highly distorted octahedron. The angles between two Mn−X bonds that are in a diagonal are 136.0° for O3−Mn−N2, 150.2° for N1−Mn−Ow1, and 170.8° for O1−Mn−O5. The six-coordination geometry in this metal chelate is, therefore, better described as a quasi-trigonal prism, although it is highly distorted from the ideal D_{3h} symmetry. The coordination geometry is similar to that in [Co_2(24edtaen)(H_2O)$_2$] in which (24edtaen)H_4 is a 24-membered macrocycle with two edta units and two en units linked by four amide bonds.[15] In these complexes, the coordination geometries are defined by the conformation of the ligand molecules.

Formation Constants. The formation constants of the complexes in Table 7 are defined as

(15) Inoue, M. B.; Inoue, M.; Fernando, Q. *Inorg. Chim. Acta* **1993**, *209*, 35.

Table 5. Fractional Coordinates and Equivalent Isotropic Temperature Factors of [Mn(13edtapn)(H_2O)]$_2$·7H_2O

atom	*x*	*y*	*z*	B_{eq},[a] Å^2
Mn	0.7508(1)	0.10023(8)	0.29638(9)	2.98(3)
O1	0.6838(4)	0.1510(4)	0.1898(4)	3.2(2)
O2	0.5796(5)	0.0234(5)	0.2719(5)	4.9(2)
O3	0.8483(5)	0.1849(4)	0.3116(5)	4.1(2)
O4	0.9759(5)	0.2161(5)	0.2794(7)	6.8(2)
O5	0.7981(5)	0.0436(4)	0.4072(5)	3.8(2)
O6	0.8161(4)	−0.0622(4)	0.4861(4)	3.4(2)
N1	0.8374(5)	0.0851(4)	0.1750(5)	2.5(2)
N2	0.7437(6)	−0.0350(4)	0.2653(5)	2.8(2)
N3	0.5819(5)	0.0130(5)	0.1235(5)	3.1(2)
N4	0.6754(5)	0.1643(4)	0.0419(5)	2.8(2)
C1	0.7158(6)	0.1497(5)	0.1147(6)	2.4(2)
C2	0.8084(6)	0.1371(6)	0.1058(7)	3.3(2)
C3	0.8368(8)	0.0042(6)	0.1456(7)	3.6(3)
C4	0.8234(7)	−0.0496(5)	0.2219(7)	3.4(3)
C5	0.6750(7)	−0.0626(6)	0.2086(7)	3.4(2)
C6	0.6078(7)	−0.0038(6)	0.2041(7)	3.1(2)
C7	0.5142(7)	0.0680(6)	0.1070(7)	3.7(3)
C8	0.5307(7)	0.1187(6)	0.0264(7)	3.8(3)
C9	0.5891(6)	0.1845(6)	0.0391(8)	3.5(2)
C10	0.9195(7)	0.1090(6)	0.2070(8)	4.1(3)
C11	0.9136(7)	0.1759(6)	0.2704(8)	4.0(3)
C12	0.7401(8)	−0.0717(6)	0.3530(6)	3.4(2)
C13	0.7886(7)	−0.0278(6)	0.4197(7)	2.9(2)
Ow1	0.6785(5)	0.1735(4)	0.3828(4)	3.5(2)
Ow2	0.250	0.250	0.280(1)	7.4(4)
Ow3	0.1109(7)	0.2516(8)	0.1793(7)	9.4(3)
Ow4	0.1766(8)	0.2833(6)	−0.002(1)	15.5(4)
Ow5[b]	0.048(1)	0.918(1)	0.061(1)	8.4(5)
Ow6[b]	0.058(1)	0.306(1)	0.400(1)	7.2(5)

[a] $B_{eq} = (4/3)[a^2\beta_{1,1} + b^2\beta_{2,2} + c^2\beta_{3,3} + ab(\cos\gamma)\beta_{1,2} + ac(\cos\beta)\beta_{1,3} + bc(\cos\alpha)\beta_{2,3}]$. [b] Occupancy = 0.5.

$$K_{ML} = \frac{[ML]}{[M][L]} \qquad M^{2+} + L^{2-} \rightleftarrows [ML]^0 \qquad (1)$$

$$K_{MLH} = \frac{[MLH]}{[ML][H]} \qquad [ML]^0 + H^+ \rightleftarrows [MLH]^+ \qquad (2)$$

$$K_{MLH_{-1}} = \frac{[MLH_{-1}][H]}{[ML]} \qquad [ML]^0 \rightleftarrows [MLH_{-1}]^- + H^+ \qquad (3)$$

$$K_{MLH_{-2}} = \frac{[MLH_{-2}][H]}{[MLH_{-1}]} \qquad [MLH_{-1}]^- \rightleftarrows [MLH_{-2}]^{2-} + H^+ \qquad (4)$$

Most of the titration curves in the basic region were characteristic of the formation of hydroxy complexes. An amide group, however, may be deprotonated at high pH, and the resulting negatively charged nitrogen may be coordinated to a metal ion.[16−18] If such a deprotonation occurs, hydroxy complexes are not necessarily formed. In eqs 3 and 4, complexes formed are given by general formulas: [MLH_{-n}] means either [ML(OH)$_n$] or [ML^{-2-n}] (L^{-2-n} is a ligand with deprotonated amide groups).

(16) (a) Bell, J. D.; Freeman, H. C.; Wood, A. M.; Driver, R.; Walker, W. R. *J. Chem. Soc., Chem. Commun.* **1969**, 1441. (b) Kimura, E.; Koike, T.; Shiota, T.; Iitaka, Y. *Inorg. Chem.* **1990**, *29*, 4621.

(17) (a) Kodama, M.; Kimura, E. *J. Chem. Soc., Dalton Trans.* **1979**, 325. (b) Kodama, M.; Kimura, E. *J. Chem. Soc., Dalton Trans.* **1981**, 694. (c) Kimura, E. *Tetrahedron* **1992**, *48*, 6175. (d) Kodama, M.; Yatsunami, T.; Kimura, E. *J. Chem. Soc., Dalton Trans.* **1979**, 1783. (e) Kimura, E.; Dalimunte, C. A.; Yamashita, A.; Machida, R. *J. Chem. Soc., Chem. Commun.* **1985**, 1041. (f) Di Casa, M.; Fabbrizzi, L.; Perotti, A.; Puggi, A.; Tundo, P. *Inorg. Chem.* **1985**, *24*, 1610. (g) Kimura, E. *J. Coord. Chem.* **1986**, *15*, 1.

(18) (a) Toki, T.; Mikuriya, M.; Okawa, H.; Murase, I.; Kida, S. *Bull. Chem. Soc. Jpn.* **1984**, *57*, 2098. (b) Hiratani, K.; Kasuga, K.; Hirose, T.; Taguchi, K.; Fujiwara, K. *Bull. Chem. Soc. Jpn.* **1992**, *65*, 2381.

Table 6. Selected Bond Distances (Å) for $[Mn(13edtapn)(H_2O)]_2 \cdot 7H_2O$

$Mn-O1_{amide}$	2.142(7)	$Mn-N1_{amine}$	2.335(8)
$Mn-O2_{amide}$	3.122(9)	$Mn-N2_{amine}$	2.411(7)
$Mn-O3_{carboxylate}$	2.185(8)	Mn−Ow1	2.178(7)
$Mn-O5_{carboxylate}$	2.096(7)		
$N3_{amide}-C6$	1.32(1)	$N4_{amide}-C1$	1.31(1)
$N3_{amide}-C7$	1.49(1)	$N4_{amide}-C9$	1.45(1)

Table 7. Logarithm of Metal−Ligand Formation Constants, log K_{MLH_n}[a]

	ML	MLH	MLH_{-1}	MLH_{-2}	σ[b]
Mn−12edtaen[c]	5.07	3.52			0.03
Mn−13edtapn[c]	5.10	3.37			0.009
Co−12edtaen	8.79	2.15	−9.52	−12.23	0.006
Co−13edtapn	8.79	2.52	−10.62	−10.26	0.006
Ni−12edtaen	11.27	1.55	−9.30	−13.90	0.005
Ni−13edtapn	10.08	1.60	−10.68	−9.78	0.003
Cu−12edtaen	11.34	1.29	−7.30	−10.41	0.006
Cu−13edtapn	10.46	1.09	−7.38	−6.05	0.009
Zn−12edtaen	8.98	1.47	−9.56	−11.94	0.003
Zn−13edtapn	9.13	2.36	−9.97	−11.24	0.01

[a] $K_{ML} = [ML]/[M][L]$; $K_{MLH} = [MLH]/[ML][H]$; $K_{MLH_{-1}} = [MLH_{-1}][H]/[ML]$; $K_{MLH_{-2}} = [MLH_{-2}][H]/[MLH_{-1}]$. pH range studied is 2.6−11.0; the number of data points is 42 ± 4; the estimated uncertainty of the log K values is ±0.03 for the primary species and ±0.05 for the secondary species. [b] σ pH fit. [c] The $K_{MLH_{-1}}$ and $K_{MLH_{-2}}$ values could not be determined accurately for Mn^{2+}, due to the formation of a precipitate in the high-pH region: the curve fits were performed with 20 data points in the pH range 3.1−5.3.

Stability constants of the ML species follow the expected pattern, based on the combined effect of central metal ion sizes and ligand field stabilization energies.[19] For Cu^{2+} and Ni^{2+} chelates, the ligand with a smaller ring size forms chelates with higher stabilities, whereas the other metal chelates of the two ligands have almost identical stabilities. The complexes formed in the basic region have the following novel properties: the formation constants of MLH_{-2} for the $(12edtaen)^{2-}$ metal chelates are smaller than the formation constants of MLH_{-1}. In contrast, for most $(13edtapn)^{2-}$ metal chelates, the formation constants of MLH_{-2} are greater than the formation constants of the corresponding MLH_{-1} species. It is reasonably certain that, in these chelates, stepwise deprotonation does not occur at high pH; if stepwise deprotonation did occur, the second stepwise dissociation or deprotonation constant should be very close to the value of the first stepwise deprotonation constant.

Electronic Spectra. The absorption maxima of the solution spectra in the visible region are collected in Table 1. An aqueous solution of Co(13edtapn) exhibited an absorption band at 510 nm ($\epsilon \sim 30$ M^{-1} cm^{-1}) with a weak shoulder on the shorter wavelength side. The nature of this spectrum is similar to that observed for the binuclear $Co^{2+}-(24edtaen)^{4-}$ complex, in which the coordination geometry around the central metal ion is a trigonal prism. The spectrum of Ni(13edtapn) showed three weak bands at 380 ($\epsilon \sim 16$), 605 ($\epsilon \sim 9$), and 1020 nm ($\epsilon \sim 20$), as shown in Figure 3. The Cu(13edtapn) complex exhibited a broad band centered at 700 nm ($\epsilon \sim 70$). These spectra are similar to the spectra that have been reported for the corresponding octahedral complexes.[20] For the corresponding metal complexes with $(12edtaen)^{2-}$, essentially identical spectra were observed. The X-ray crystal analyses of Zn(12edtaen), Mn(13edtapn), and Cu(12edtaen) have shown that both ligands can occupy five of the six coordination sites on the central metal ions. Polymeric chelates of the Cu^{2+} and Zn^{2+} complexes that are obtained as solids are dissociated to monomeric molecules in solution, and the oxygen atom from the neighboring chelate molecule is replaced by an oxygen atom from a water molecule in each monomer. In solution, therefore, the five coordinating atoms of a ligand molecule, together with an oxygen atom from a water molecule, form a distorted octahedron or trigonal prism around a central metal ion. The six-coordination geometry of these complexes is consistent with the observed solution spectra. Six-coordinated Co^{2+} and Ni^{2+} complexes are usually in the high-spin state.[21] This is confirmed by the magnetic moments (Table 1) of the solid samples for the Co^{2+} and Ni^{2+} complexes of the new macrocyclic ligands.

During the potentiometric titration of solutions containing $(13edtapn)H_2$ and Ni^{2+} or Cu^{2+}, dramatic color changes were observed. The solution containing Ni^{2+} changed from green at low pH to yellow at high pH, and the solution containing Cu^{2+} changed from pale blue to deep purple. The spectra of Ni(13edtapn) at different pH values are shown in Figure 3. With increasing pH, the three absorption bands weakened, and a new band formed at 470 nm. At pH ≥ 10, only the 470 nm band was observed: the molar absorptivity of the new band was ~117 at pH = 11.0. Similar changes in the spectrum of a nickel(II) complex with triethylenetetramine have been reported.[22] An aqueous solution of this complex in the presence of nitrate ions showed absorption bands at 358 and 564 nm. When sodium perchlorate was added to the solution, a new band appeared at 443 nm and increased in intensity with increasing sodium perchlorate concentration. These spectral changes are the result of a change in the coordination geometry from octahedral to square planar.[22] Thus, solution electronic spectroscopy is an empirically established diagnostic method for determination of the coordination geometries of Ni^{2+} chelates in solution. Since $[NiLH_{-2}]$ at pH = 11.0 is calculated to be 92% for the $(13edtapn)H_2$ complex on the basis of the potentiometric titration data, the spectrum observed at pH 11.0 indicates that $NiLH_{-2}$ species has a square planar structure. The formation constant of the $NiLH_{-1}$ species is smaller than that of $NiLH_{-2}$ species, and $[NiLH_{-1}]$ is only 15% even at pH = 10.2 where $[NiLH_{-1}]$ is at a maximum. The spectrum due to $NiLH_{-1}$ is, therefore, masked by the spectra of the other species. The spectrum of Ni(12edtaen) at neutral pH closely resembled that of Ni(13edtapn) but showed neither significant shift nor absorptivity change with pH in the visible region (Figure 3). The only significant variation with pH was observed in the near-infrared region: the 1020 nm band disappeared at high pH, and a diffuse envelope was observed without a well-defined peak. Since the log $K_{NiLH_{-2}}$ of Ni(12edtaen) is very small and only $NiLH_{-1}$ is formed even at pH = 13.0 where the spectrum B is observed, the $NiLH_{-1}$ species is deduced to have essentially the same coordination geometry as that of the NiL species. In the spectra of Cu(13edtapn), the band of $\lambda = 700$ nm ($\epsilon \sim 70$) at pH 5.8 showed a large blue shift and increased in intensity with increasing pH: at pH = 6.7, $\lambda = 603$ nm and $\epsilon \sim 120$; at pH = 7.5, $\lambda = 570$ nm and $\epsilon \sim 205$; at pH = 12.8, $\lambda = 570$ nm and $\epsilon \sim 215$. It is well-known that a blue shift with an increase in the molar absorptivity is observed for copper(II) complexes when coordinated oxygen atoms (such as water oxygen atoms) are replaced by nitrogen atoms from other ligands (such as ammonia).[20] Comparison of the species distribution diagram and the spectral change observed for Cu(13edtapn) shows that the number of coordinated nitrogen atoms in $CuLH_{-2}$ is greater than that in CuL and the two species have different coordination geometries: $[CuL] \sim 97\%$ at pH = 5.8, and $[CuLH_{-2}] \sim 100\%$

(19) Dunn, T. M.; McClure, D. S.; Pearson, R. G. *Some Aspects of Crystal Field Theory*; Harper & Row: New York, 1965; p 77.
(20) Cotton, F. A.; Wilkinson, G. *Advanced Inorganic Chemistry*, 5th ed.; Wiley Interscience: New York, 1988; pp 649, 770.
(21) Casey, A. T.; Mitra, S. In *Theory and Applications of Molecular Paramagnetism*; Boudreaue, E. A., Mulay, L. N., Eds.; John Wiley: New York, 1976; p 135.
(22) Jørgensen, C. K. *Acta Chem. Scand.* **1957**, *11*, 399.

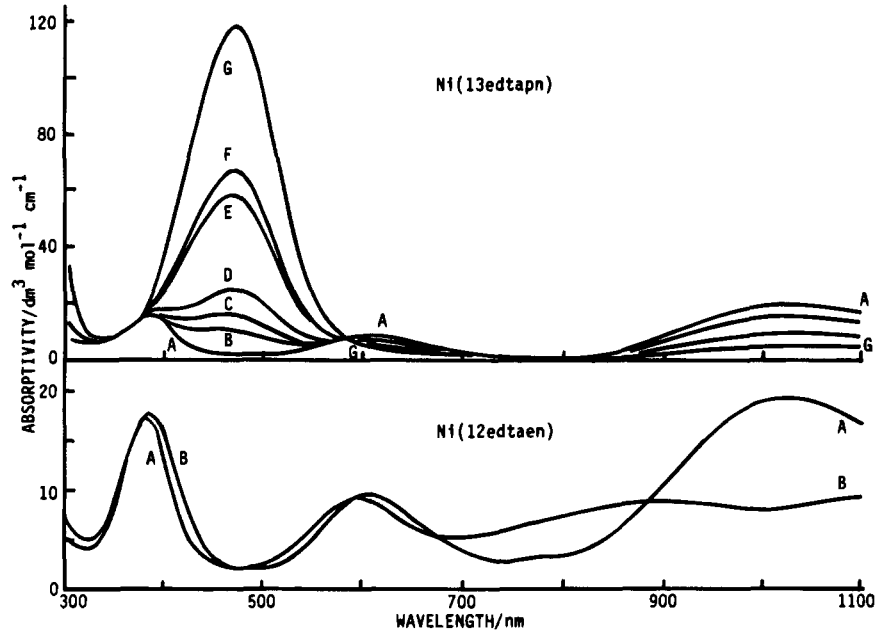

Figure 3. Solution spectra in the visible region of Ni(12edtaen) at pH = 7.8 (A) and 13.0 (B) and spectra of Ni(13edtapn) at pH = 6.4 (A), 9.1 (B), 9.4 (C), 9.5 (D), 10.1 (E), 10.2 (F), and 11.0 (G).

Scheme 1

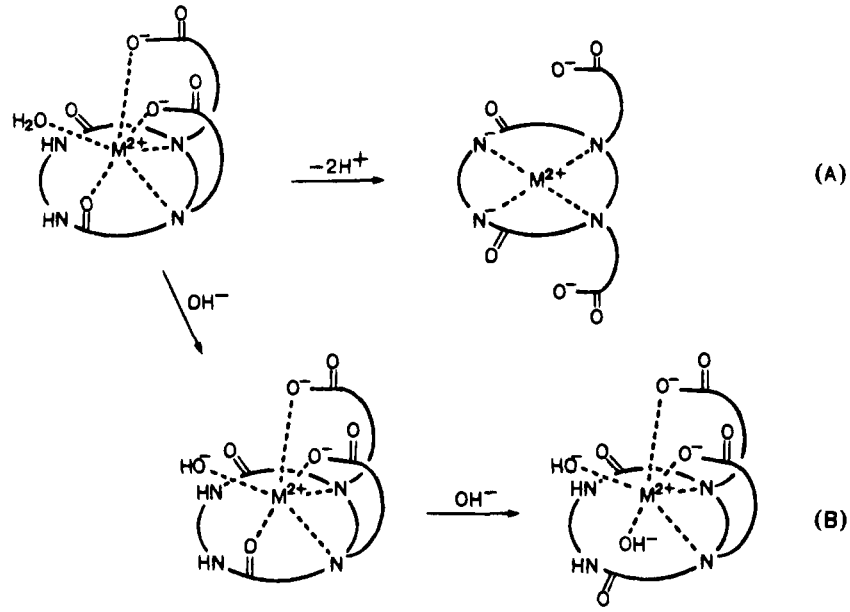

at pH = 12.8. In the spectrum of Cu(12edtaen), the 745 nm band ($\epsilon \sim 45$) observed at pH = 5.5 showed a blue shift with increasing pH. The extent of the shift was, however, much smaller than that of Cu(13edtapn), and the change in the molar absorptivity was not significant: at pH = 8.9, λ = 708 nm and $\epsilon \sim 40$; at pH = 12.8, λ = 670 nm and $\epsilon \sim 50$. The formation of Cu(12edtaenH$_{-n}$) species is almost stepwise. Comparison of the species distribution diagram and the solution spectra shows the following: the spectrum at pH = 5.5 is due to the CuL species (~97%); the spectrum at pH = 8.9 to CuLH$_{-1}$ (~95%); the spectrum at pH = 12.8 to CuLH$_{-2}$ (100%). This result indicates that the number of coordinated nitrogen atoms is not changed with pH in Cu(12edtaen), even for the CuLH$_{-2}$ species in contrast to Cu(13edtapn).

The pH dependence of the electronic spectra of the Ni^{2+} and Cu^{2+} complexes suggests that reactions with OH^- proceed differently for the $(12edtaen)^{2-}$ and $(13edtapn)^{2-}$ complexes. This observation is related to the formation constants of the basic species of the complexes: for the $(13edtapn)^{2-}$ complexes, the stability constants of the MLH$_{-2}$ species are greater than those of the corresponding MLH$_{-1}$ species, whereas the reverse relation exists for the $(12edtaen)^{2-}$ complexes. In the literature we can find several instances in which, at high pH, an amide group is deprotonated and the resulting negatively charged nitrogen is coordinated to a Cu^{2+} ion in place of an amide oxygen atom.[16-18] The spectral changes observed for the $(13edtapn)^{2-}$ complexes indicate that such a deprotonation of amide groups occurs in the species CuLH$_{-2}$ (Scheme 1A), in which two negatively charged amide nitrogen atoms together with two amine nitrogen atoms are coordinated to the central metal ion, thereby forming a square planar structure. Carboxylate oxygen atoms are weakly coordinated to the central metal ion in a CuLH$_{-2}$ molecule and are out of the first coordination sphere in a NiLH$_{-2}$ molecule. The concentration of the MLH$_{-1}$ species is very low throughout the basic region. This species is converted to MLH$_{-2}$ in such a manner that two amide groups in a metal chelate molecule can be considered to be deprotonated simultaneously. On the other hand, the electronic spectra of

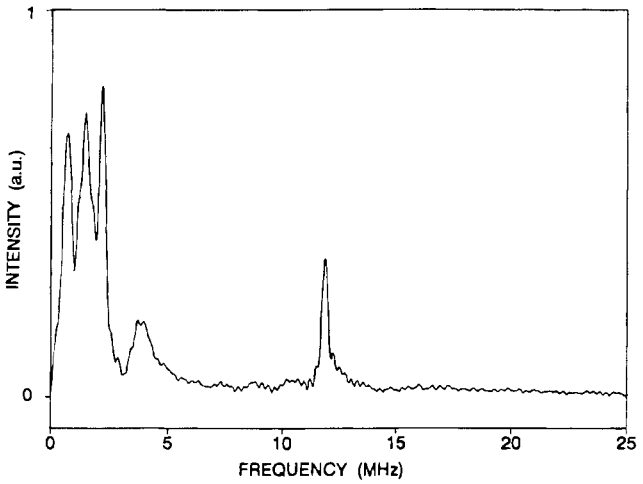

Figure 4. FT-ESEEM (stimulated echo) spectrum observed for Cu(13edtapn) in an acidic matrix. The experimental conditions were as follows: temperature = 4.2 K; microwave frequency = 8904 MHz; magnetic field = 2794 G (I(Cu) = $^1/_2$); τ = 300 ns.

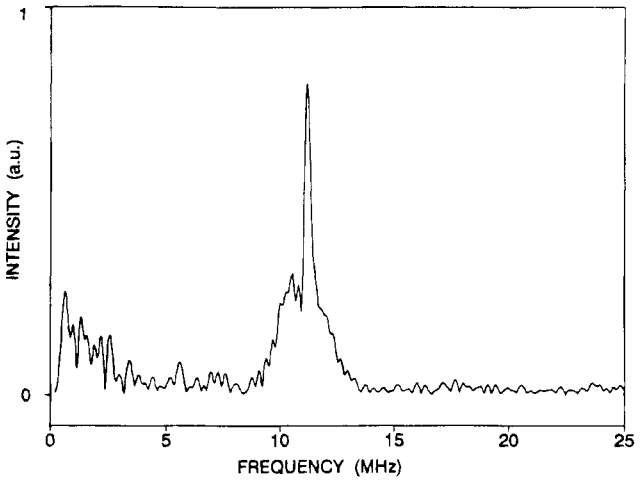

Figure 5. FT-ESEEM (stimulated echo) spectrum observed for Cu(13edtapn) in a basic matrix. The experimental conditions were as follows: temperature = 7 K; microwave frequency = 8904 MHz; magnetic field = 3632 G (I(Cu) = $-^3/_2$); τ = 356 ns.

the $(12edtaen)^{2-}$ complexes indicate that a deprotonation of an amide group does not occur, but $ML(OH)_n$ species are formed instead, as shown in Scheme 1B: a water molecule coordinated in a CuL molecule is replaced by an OH^- group in a $CuLH_{-1}$ molecule, and an amide oxygen atom, which has the lowest coordination ability, is replaced by another OH^- oxygen atom in the $CuLH_{-2}$ species. When an amide oxygen atom is not coordinated to a Cu^{2+} ion, the steric constraint is decreased, and hence amine nitrogen atoms can be closer to the central metal ion, resulting in the small blue shift that was observed for Cu(12edtaen).

The 510 nm band observed for the Co^{2+} complex with $(13edtapn)H_2$ did not shift with pH. The molar absorptivity, however, distinctly increased with increasing pH: $\epsilon \sim 30$ at pH = 7.1; ~55 at pH = 10.2; ~115 at pH = 12.7. The absorption spectrum of the Co^{2+} complex with $(12edtaen)H_2$ consists of two component peaks at 490 and 510 nm. The molar absorptivity of the latter band was 18 and constant throughout the pH range studied. The 490 nm band strengthened at high pH, but the increase of the absorptivity was not significant: $\epsilon \sim 18$ at pH = 7.9 and 9.1; ~22 at pH = 10.1. These spectral changes suggest that the coordination mode in the $(13edtapn)H_2$ complex changes significantly with pH, whereas no significant change occurs in the $(12edtaen)H_2$ complex. The titration curves observed for the Co^{2+} complexes are quite similar to the corresponding curves observed for the Ni^{2+} complexes. The pH effect on the coordination geometry in the Co^{2+} complexes is, therefore, similar to that in the corresponding Ni^{2+} complexes.

Electron Spin Echo Envelope Modulation (ESEEM) Spectra. ESEEM experiments were carried out for Cu(13edtapn), with the objective of confirming the coordination of deprotonated amide nitrogen atoms to a Cu^{2+} ion in basic solutions. The Fourier-transformed stimulated ESEEM spectra are shown for the acidic and basic matrices in Figures 4 and 5, respectively. ESEEM can be observed only for a nucleus having a weak I-S coupling whose energy is of the same order of magnitude as the nuclear Zeeman energy and the nuclear quadrupole energy.[23] The FT ESEEM spectra of copper–imidazole complexes and analogues, for example, show a series of peaks at frequencies below 5 MHz, and these peaks are attributed to "remote" nitrogen atoms that are not directly coordinated to a Cu^{2+} ion,[23,24] because only a nitrogen atom having a weak interaction with a Cu^{2+} electron spin gives well-defined ESEEM. The spectrum of the acidic matrix (Figure 4) is very similar to the spectra obtained for the Cu–imidazole complexes; a series of peaks observed at frequencies below 5 MHz are attributable to remote nitrogen, and a peak at 12 MHz to hydrogen. It is reasonable that Cu(13edtapn) in an acidic matrix has essentially the same structure as in the solid: two amine nitrogen atoms are directly coordinated to a Cu^{2+} ion, and amide nitrogen atoms are not coordinated to the metal ion. The nitrogen peaks in the ESEEM spectrum of the acidic matrix (Figure 4), therefore, can be attributed to amide nitrogen. In the spectrum of the basic matrix (Figure 5), no nitrogen peak was detected in contrast to the acidic matrix. This suggests that the amide nitrogen atoms together with the amine nitrogen atoms are directly coordinated to a Cu^{2+} ion in basic solutions. The ESEEM experiments provided additional evidence for Scheme 1A.

The ESR spectrum of Cu(13edtapn) in a glass matrix made from an acidic solution at liquid nitrogen temperature showed the g tensor: $g_1 = 2.336$ (A_1(Cu) = 147 G), $g_2 = 2.073$, and $g_3 = 2.039$. The g values determined in a basic matrix are $g_{||} = 2.190$ ($A_{||}$(Cu) = 188 G) and $g_\perp \sim 2.0$; this spectrum showed a structure at $g \sim 2$ due to a nonmonotonous spectrum function,[25] and hence the $g_\perp$ value could not be accurately determined. The g values of Cu^{2+} complexes with an elongated D_{4h} ligand field have been given by[26]

$$g_{||} = 2.0023 + 8\lambda_{LS}/\Delta E(d_{x^2-y^2} - d_{xy}) \quad (5)$$

$$g_\perp = 2.0023 + 2\lambda_{LS}/\Delta E(d_{x^2-y^2} - d_{yz,zx}) \quad (6)$$

where λ_{LS} is the spin–orbit coupling constant. An increase in the strength and/or the elongation of a D_{4h} ligand field leads to the increase of the energy differences, $\Delta E(d_{x^2-y^2} - d_{xy})$ and $\Delta E(d_{x^2-y^2} - d_{yz,zx})$, and consequently the g values are closer to 2.0023.[26] The g values in the alkaline matrix are closer to 2.0023 than are the corresponding values in the acidic matrix. This is consistent with the structural change deduced for Cu-

(23) Thomann, H.; Mims, W. B. In *Pulsed Magnetic Resonance: NMR, ESR and Optics*; Bagguley, D. M. S., Ed.; Oxford University Press: New York, 1992; p 362.

(24) (a) Jiang, F.; McCracken, J.; Peisach, J. *J. Am. Chem. Soc.* **1990**, *112*, 9035. (b) Goldfarb, D.; Fauth, J.-M.; Tor, Y.; Shanzer, A. *J. Am. Chem. Soc.* **1991**, *113*, 1941.

(25) Neiman, R.; Kivelson, D. *J. Chem. Phys.* **1961**, *35*, 156.

(26) Goodman, B. A.; Raynor, J. B. In *Advances in Inorganic Chemistry and Radiochemistry*; Emeléus, H. J., Sharpe, A. G., Eds.; Academic Press: New York, 1970; p 313.

(13edtapn) on the basis of the solution electronic spectra and the ESEEM data.

Discussion

The X-ray, magnetic, and spectroscopic data indicate that the ML species of the series of the complexes have a six-coordination geometry, which is either a distorted octahedron or a distorted trigonal prism. The Mn^{2+} and Zn^{2+} complexes have no crystal field stabilization, and the formation constants of the complexes of the two ligands are practically identical. The formation constants of the Ni^{2+} and Cu^{2+} complexes with $(12edtaen)^{2-}$ are greater than the formation constants of the corresponding complexes with $(13edtapn)^{2-}$. The partial double-bond character of the amide C−N bonds (Tables 4 and 6) reduces the flexibility of the macrocyclic rings and defines the conformation of the ligand molecule. The conformation of the ligand, $(12edtaen)^{2-}$, favors the formation of the Cu^{2+} and Ni^{2+} complexes that are stabilized by ligand field energies.

The introduction of an amide group into the ring system reduces the basicity of amine nitrogen.[4] As a result, the formation constants of the ML species are smaller than the corresponding values of the complexes with tetraazamacrocycles and their carboxymethyl derivatives: logarithms of the formation constants of ML species of 1,4,7,10-tetraazacyclododecane (**III**) are 23.29[27d] −24.8[27a] for Cu^{2+}, 16.4[27d] for Ni^{2+}, and 16.2[27c] for Zn^{2+}; log K_{ML} values of 1,4,7,10-tetraazacyclotridecane (**IV**) are 24.36[27d]−29.1[27b] for Cu^{2+}, 17.98[27d] for Ni^{2+}, and 15.6[27c] for Zn^{2+}; log K_{ML} values of the tetrakis(*N*-(carboxymethyl)) derivative (**V**) of **III** are 19.06 for Cu^{2+}, 17.25 for Ni^{2+}, and 18.90 for Zn^{2+};[27f] log K_{ML} values of the tetrakis(*N*-(carboxymethyl)) derivative (**VI**) of **IV** are 17.29 for Cu^{2+}, 15.75 for Ni^{2+}, and 14.42 for Zn^{2+}.[27f] A 2,6-dioxo derivative (**VII**) of **III** and a 11,13-dioxo derivative (**VIII**) of **IV** do not form ML species; instead, MLH_{-2} species are formed even in the neutral region. The formation of ML species with $(12edtaen)H_2$ and $(13edtapn)H_2$ is due to the coordination of *N*-(carboxymethyl) groups.

The occurrence of Scheme 1A or 1B in the Ni^{2+} and Cu^{2+} complexes can be explained by the difference in the ring size of the ligands. The formation constants of Ni^{2+} and Cu^{2+} chelates with tetraazacyclododecane (**III**) are significantly smaller than the corresponding constants for tetraazacyclotridecane (**IV**).[27] The tridecane ring favors the formation of a square planar coordination geometry around a central metal ion, but the dodecane ring is too small to accommodate a metal ion in its cavity. This size effect is notable in the $(12edtaen)^{2-}$ and $(13edtapn)^{2-}$ chelates and results in the formation of different species as shown in Scheme 1. The selectivities of the ligands toward specific metal ions are pH-dependent and are enhanced in the basic region.

The dioxotetraazacyclotridecane **VIII** forms MLH_{-2} complexes with Cu^{2+} and Ni^{2+}, in which amide groups are deprotonated, and the mode of coordination is expected to be similar to that in the Cu^{2+} and Ni^{2+} complexes with $(13edtapnH_{-2})$. The logarithm of the cumulative formation constant is −2.2 for Cu−**VIII**,[17a] −6.0 for Ni−**VIII**,[17b] −2.97 for $Cu(13edtapnH_{-2})$, and −10.38 for $Ni(13edtapnH_{-2})$. The difference in the stabilities of the two series of complexes reflects the effect of coordination of carboxylate groups in the $(13edtapnH_{-2})$ complexes. The stabilities of Cu^{2+} complexes are almost identical, whereas $Ni(13edtapnH_{-2})$ is significantly less stable than Ni−**VIII**. A square planar Ni^{2+} complex has a large ligand field stabilization energy. The location of additional axial donor atoms decreases the stabilization energy, even when the coordination of the axial donors is very weak as demonstrated for the $(13edtapnH_{-2})$ complex by its visible spectrum. In contrast, the coordination of axial donors is less effective for a Cu^{2+} complex that has an electron configuration of $3d^9$. Since a tetraazadodecane ring is too small to accommodate a metal ion in its cavity, its metal complex has a relatively low stability constant. The coordination of carboxylate oxygen atoms does not decrease the ligand field stabilization energy but increases the stability due to increase in the number of coordinated donor atoms. Therefore, the $(12edtaenH_{-2})$ complexes with Cu^{2+} and Ni^{2+} are more stable than the corresponding complexes of the dioxotetraazacyclododecane **VII**: the logarithm of the cumulative formation constant is −6.37 for $Cu(12edtaenH_{-2})$, −9.2 for Cu-**VII**,[17b] −11.93 for $Ni(12edtaenH_{-2})$, and −13.0 for Ni−**VII**.[17b]

For Zn(12edtaen) and Zn(13edtapn), the formation constants of the MLH_{-2} species are smaller than those of the corresponding MLH_{-1} species. Both the Zn complexes behave in accordance with Scheme 1B, in which the hydroxy complexes are formed in the basic region. For a Zn complex, there is no increase in the crystal field stabilization energy by changing from an octahedral structure to a planar structure, and a Zn^{2+} complex with tetraazacyclotridecane (**IV**) is less stable than a Zn^{2+} complex with tetraazacyclododecane (**III**),[27] in contrast to the case for Ni^{2+} and Cu^{2+}. This is the reason that the behavior of Zn(13edtapn) is different from the corresponding Ni^{2+} and Cu^{2+} complexes.

It is noteworthy that the differences between the $(12edtaen)^{2-}$ and $(13edtapn)^{2-}$ complexes of Co^{2+}, Ni^{2+}, and Cu^{2+} are caused by the difference of only one $-CH_2-$ group in the rings of the ligands. The molecular structures of the Gd^{3+} chelates of 15-membered and 16-membered dioxopentaazacycloalkanetriacetates are quite different from each other. The complex with the ligand that has a 15-membered ring has a binuclear structure whereas the complex with the ligand that has a 16-membered ring has a mononuclear structure.[28] This difference is also caused by a difference of only one $-CH_2-$ group in the ligand ring systems. The ring-size effect of macrocyclic ligands is one of the controlling factors in selective complexation of macrocyclic ligands with metal ions. This effect is expected to be enhanced by the introduction of appropriate functional groups. The novel properties observed in this study may be related to the unique arrangement of the three types of donor atoms in the ligand molecules.

Acknowledgment. The construction of the ESEEM spectrometer was supported by the NSF (Grant No. BIR-9224431). The work at the Universidad de Sonora was supported by CONACYT, Mexico (Grant No. 2418-E9303).

Supplementary Material Available: Tables of anisotropic thermal parameters, positional and *B* parameters of hydrogen atoms, additional bond lengths and angles, least-squares planes, and intermolecular contacts and ORTEP diagrams of the unit cells for $[Zn(12edtaen)]\cdot 4H_2O$ and $[Mn(13edtapn)(H_2O)]_2\cdot 7H_2O$ (14 pages). Ordering information is given on any current masthead page.

IC941369Q

(27) (a) Kodama, M.; Kimura, E. *J. Chem. Soc., Chem. Commun.* **1975**, 326. (b) Kodama, M.; Kimura, E. *J. Chem. Soc., Chem. Commun.* **1975**, 891. (c) Kodama, M.; Kimura, E. *J. Chem. Soc., Dalton Trans.* **1977**, 2269. (d) Thöm, V. J.; Hancock, R. D. *J. Chem. Soc., Dalton Trans.* **1985**, 1877. (e) Hancock, R. D.; Ngwenya, M. P. *J. Chem. Soc., Dalton Trans.* **1987**, 2911. (f) Stetter, H.; Frank, W. *Angew. Chem., Int. Ed. Engl.* **1976**, *15*, 686.

(28) Inoue, M. B.; Inoue, M.; Muñoz, I. C.; Bruck, M. A.; Fernando, Q. *Inorg. Chim. Acta* **1993**, *209*, 29.